

**DEPTH-INTEGRATED DISPERSION MODEL PREDICTION OF  
DENSE GAS DISPERSION IN THE PRESENCE OF  
BARRIERS AND WATER SPRAY CURTAINS**

by

Robert N. Meroney  
Colorado State University

Seong-Hee Shin  
EXXON Research and Engineering

Fluid Mechanics and Wind Engineering Program  
Department of Civil Engineering  
Colorado State University  
Fort Collins, Colorado 80523

Prepared for  
Symposium on Measurement and Modeling of Environmental Flows  
ASME Winter Annual Meeting  
Anaheim, California  
November 8-13, 1992

April 1992

CEP91-92-RNM-SHS-4

# DEPTH-INTEGRATED DISPERSION MODEL PREDICTION OF DENSE GAS DISPERSION IN THE PRESENCE OF BARRIERS AND WATER SPRAY CURTAINS

Robert N. Meroney, Civil Engineering Department  
Colorado State University, Fort Collins, CO

Seong-Hee Shin, Environmental Marine and Safety Division,  
EXXON Research and Engineering, Florham Park, NJ

**ABSTRACT** Accidental releases of chemicals such as hydrogen fluoride can result in initially dense gas clouds that will typically contain a mixture of gases aerosols and droplets which can be transported significant distances before lower hazard limits are reached. Containment fences, vapor barriers and water-spray curtains have been proposed as a means to hold-up of delay cloud expansion, enhance cloud dilution, and/or remove the hazardous materials from the gas cloud by deposition. This paper predicts dense plume/barrier interactions based on box and depth-integrated numerical models which includes the effects of barrier height, lateral barrier extent, barrier porosity, and water-spray dilution or deposition. The models have been validated against the Falcon Liquefied Natural Gas (LNG) barrier experiments, the Goldfish Hydrogen Fluoride (HF) water-spray experiments, and the Gas Research Institute (LNG) and Health and Safety Executive (CO<sub>2</sub>) water-spray experiments.

Freon-air mixtures at Thorney Island, the release of hydrocarbon fuels at Maplin Sands, and the release of hydrocarbon fuels, ammonia, rocket fuels, and even HF at the DOE Liquefied Gaseous Fuels Test Facility at Frenchman's Flats, Nevada. A number of these experiments have also been simulated in fluid modeling facilities (Meroney, 1986). Meroney et al. (1988) examined eleven data sets from field and laboratory experiments dealing with the influence of vapor barrier fences and water spray curtains on the dispersion of dense gas clouds. Tests were paired into sets of data which reflected the dilution of the cloud with and without the barriers present. Peak concentration ratios, cloud arrival time ratios, peak arrival time ratios, and departure time ratios were calculated for each test pair.

## INTRODUCTION

Recent disastrous accidents (e.g., Bhopal [1984], Chernobyl [1986], Kerr-McGee [1986]) have focused attention on the potential risks of large and small scale releases of flammable or toxic gases. This paper examines numerically the effectiveness of combinations of vapor barriers and water-spray curtains in diluting and delaying heavier-than-air vapor clouds. Two numerical models were equipped with entrainment algorithms which allow for the enhanced dilution or deposition caused by water spray curtains and vapor barrier fences. A continuous source box model was modified to incorporate the joint presence of fences and water sprays including the possibility of variable fence height and porosity and variable water spray velocities and deposition. A depth-averaged model was modified to include the effect of side fences which can enclose a spill area and inhibit initial lateral growth at the source.

Puttock, Blackmore and Colenbrander (1982) identified over 22 field experiment programs on dense gas emissions. Subsequently, further field measurements have been performed on the release of

## PREDICTION OF DENSE GAS DILUTION

When the flow situation is steady and diffusion in one direction is weak with respect to advection, it is possible to integrate over a plume cross-section and calculate plume width, average height, and cross-section averaged velocities, concentrations, temperatures, and humidity. Such a "box" type model is numerically very fast since the conservation equations reduce to a set of coupled ordinary differential equations. Alternatively when vapor generation is transient, and there are opportunities for upwind flow, a set of coupled partial differential equations of only two dimensions and time can be created by integrating the conservation equations over just the depth. Such a "shallow layer" or "slab" type model provides information about time- and space-dependent cloud widths, heights, and depth-averaged velocities, concentrations, temperatures, and humidities.

A box model (Meroney, et al., 1988; Meroney and Lohmeyer, 1984; Andriev et al., 1983; and Meroney and Shin, 1991) and a slab model (Meroney and Lohmeyer, 1982; Meroney, 1984; Shin and Meroney, 1991) have been adapted to consider the dilution of a hypothetical small area spill of dense gases by water sprays and vapor barrier fences (DENS70 and FENCE, respectively).



## Entrainment Models for Vapor Barriers and Water Spray Curtains

Both numerical models normally use the concept of an entrainment velocity,  $w_e$ , across the upper cloud surface to mix the cloud with ambient air. The entrainment velocity is a semi-empirical function of boundary-layer and cloud variables such that,

$$w_e = f(U_g, u_*, w_*, Ri_*), \quad (1)$$

where  $U_g$  = plume frontal velocity,  $u_*$  = friction velocity,  $w_*$  = convective velocity,  $Ri_*$  = local Richardson number. Water spray and fence entrainment effects can be included by adding the enhanced entrainment rates associated with the mitigation device to that normally present due to background turbulence and plume motion,,

$$(w_e)_{total} = w_e + (w_e)_{fence} + (w_e)_{spray}. \quad (2)$$

Reductions in cloud concentrations can also occur through chemical reaction between the cloud and water spray. For example, HF reacts with the liquid water and leaves the cloud as the water deposits on the ground. Laboratory and field tests described by Blewitt et al. (1987) measured HF removal ranging from 9 to 80%. This feature of water spray feature was added to the continuous source box models by decreasing the effective source strength immediately downwind of the spray curtain. Specific models used to relate nozzle geometry and placement to water spray curtain dilution were described earlier by Meroney and Neff (1985) and Atallah, Guzman and Shah (1988).

The following simple model was proposed to described the increased entrainment resulting from a vapor barrier fence:

$$(w_e)_{fence} = C_D U(H)(1 - P)(1 - (x - x_f)/(30H)), \quad (3)$$

where  $x$  is distance downwind of the source,  $x_f$  is fence location,  $H$  is fence height,  $U(H)$  is fence height wind speed,  $P$  is fence porosity, and the relation is not used downwind of  $x_f$ . Atallah, Guzman and Shah (1989) discuss other aspects of vapor barrier design.

## Calibration of the Water Spray Entrainment Model

Results from a laboratory program to study water-spray curtain interaction with dense gas plumes were used to check the numerical models outlined above (Heskestad, et al., 1983). Wind-tunnel spray simulations were compared against field data dispersion of carbon dioxide gas clouds in a separate test series (Meroney, Neff and Heskestad, 1984). The additive model successfully predicted plume dilutions, vertical plume growth, and plume spread over a wide combination of spray configurations (Meroney and Neff, 1985).

## Calibration of the Vapor Removal Model

Deposition measurements suggested that water sprays removed 10-25%, 44%, and 47% of the Hydrogen Fluoride during Goldfish Trials 4, 5, and 6, respectively. The water spray systems were designed to produce small droplets to enhance chemical reactions, rather than strong dilution. DENS70 was used to predict cloud concentrations with the reduction mode on but water spray entrainment set to zero (Meroney and Shin, 1991). Field conditions could be reproduced, but this module has not been subsequently compared to independent measurements.

## Calibration of the Vapor Barrier Fence Entrainment Model

Data from the pre-Falcon model tests performed by Neff and Meroney (1985) were used to calibrate the vapor barrier fence entrainment model. A value  $C_D = 0.1$  provided the best agreement. Subsequently, the fence entrainment model, FENCE, was used to predict liquefied natural gas dilution downwind of vapor barriers during the FALCON field and laboratory test series (Shin and Meroney, 1991). Predictions were equivalent within field and laboratory instrumentation accuracy. The numerical model was also used to evaluate the relative impact of molecular diffusion on model scale tests, and it was concluded molecular dispersion (Pe/Ri Ratio) effects are small when model buildings or barriers are present.

## RELATIVE PERFORMANCE OF FENCE AND WATER SPRAY BARRIERS

Meroney and Neff (1985) examined the effect of a hypothetical water spray barrier on the Burro No. 8 LNG field tests. Meroney and Shin (1991) reported the impact of different fences and water spray barriers on the Goldfish No. 1 Hydrogen Fluoride field test. Other dense gas spill configuration were proposed and tested in the API Publication No. 4491 (1989) to evaluate the relative impact of surface roughness on heavier-than-air dispersion. Two run cases, Test 29 and 30, simulated the release of heavy gas ( $SG = 1.4$  and  $4.0$ , respectively) at a release rate of  $Q = 11.14 \text{ m}^3/\text{s}$  from a small 5 m diameter area source over a surface roughness,  $Z_o = 0.03$  m, at a wind speed of  $U_{10} = 5.6 \text{ m/s}$ . These conditions have been chosen for further evaluation given the hypothetical addition of fence and/or water spray barriers. Numerical calculations were also performed for a reduced wind speed of  $U_{10} = 3.0 \text{ m/s}$ .

## Fence Barriers

During numerical sensitivity tests reported earlier (Meroney and Shin, 1991) the effects of fence location were determined to be similar to that of water spray curtain location. Fences are more effective in terms of initial dilution, when they are placed nearer the source. Fence dilution effects did not persist beyond 1000 m, when the fence was placed less than 400 m downwind of the source.

The fence entrainment model permits the entrainment velocity to increase with fence height velocity. Since wind profiles increase with height, then the dilution rate should increase with fence height. The box model assumes that a logarithmic velocity profile exists, such that wind speed is determined by surface roughness and friction velocity. The entrainment velocity does not turn off abruptly like the water spray model, but decreases linearly out to a distance of 30 fence heights. The resulting displacement of the concentration profile is cusp shaped rather than triangular, and the dilution effect is small after about 200 fence heights. The cloud height approaches the cloud height in the absence of a barrier after 1000 meters or about 200 fence heights.

Increased wind speeds result in larger entrainment rates, but this is compensated by the tendency for the plume to pass through the fence wake more quickly. Given a constant fence height of 3 meters located 100 meters downwind of the source for a range of wind speeds varying from 1 to 8 m/sec, the increased entrainment and shortened time in the wake balance out to produce no net change in dilution rate. Plume height also remains constant. These



calculations agree with other experiences in building aerodynamics, where it is found that perturbation of gas plumes by obstacles seems to be velocity independent. Concentrations decay at higher wind speeds inversely with the speed, but this is an independent effect of source dilution by the ambient wind, not an effect of a fence.

Cloud height downwind of an obstacle is expected to be independent of wind speed, since a sharp edged geometry will produce similar streamline patterns over a range of velocities. Model results suggest that the perturbation produced by a fence is constant, but the model fails to allow for a constant height wake region.

Figure 1 compares the relative dilutions and plume growth of a 1.4 specific gravity plume for wind speeds of 3.0 and 5.6 m/s, barrier heights of 2, 4, and 6 m, and barrier porosities of 0 and 50 %. All barriers were located 20 m downwind of the source area. As before increases in wind speed and barrier height increase dilution. An increase in barrier porosity decreases plume dilution by one-third. The barriers diluted a denser plume of 4.0 specific gravity slightly more effectively, primarily because the increased entrainment acted over a greater surface area due to enhanced plume width at the fence location, Figure 2.

#### Water Spray Curtain Barriers

The box model was also used to predict the joint effects of water spray dilution and deposition on an HF cloud (Meroney and Shin, 1991). Spray deposition produces a parallel shift of the concentration decay curve. A second spray produces a second shift of equivalent width. The decrease in concentration persists at all subsequent downstream distances.

Alternatively consider the dilution effect of the water sprays. Separate calculations considered the effect of varying curtain location from 30 to 400 meters downwind of the spill center. A nominal spray entrainment rate of 6 m/sec was chosen for these calculations. The concentrations predicted downwind of the spray location were very similar with just slightly lower concentrations when the spray is further downwind. The magnitude of the reduction in concentrations when the barrier is farther from the source is not large, and any advantage in final concentrations would be outweighed by the greatly increased water consumption as the spray curtain width increases over the wider plume.

Other calculations examined the effect of a water spray curtain on plume height when activated at various downwind distances. Near the source cloud height is increased 25-fold; whereas further downwind the same spray curtain only causes a 2.5-fold increase in height. Given a constant spray location, wind speed, and plume width, increased entrainment velocities result in proportional increases in dilution.

Increased wind speed advects the gas plume through the spray zone more quickly. Given a constant water spray entrainment rate of 6 m/sec, then a plume moving slowly through the spray curtain at 1 m/sec will receive about 12.5 times more dilution than a plume traveling at 10 m/sec. Cloud height increases by the same ratio.

Figure 3 compares the relative dilution and plume growth behavior of a 1.4 and 4.0 specific gravity plume downwind of our generic small-area source spill for a wind speed of 3.0 m/s when a water spray with entrainment velocities of 0, 1, 2, and 5 m/s and deposition strengths of 0, 50 and 75 %. All water spray curtains were located 20 m downwind of the source area. As before an

increase in water spray entrainment velocity increases dilution proportionally, and deposition results in a permanent shift of downwind concentrations to lower values. The mitigation devices are slightly more effective when interacting with a 4.0 specific gravity plume, primarily because the water spray curtain acts over a greater plume width at the spray location.

#### JOINT PERFORMANCE OF FENCE AND WATER SPRAY BARRIERS

Meroney and Neff (1985) previously described the effect of dual water spray barriers. When both barriers operated with the same entrainment rates, the net effect of two such barriers located downwind of one another seems to be very close to the effect expected from one barrier with twice the entrainment velocity. The second barrier must also be wider in order to intercept over a wider plume; hence, greater water consumption may occur. Meroney and Shin (1991) reported the effect of dual water sprays including deposition. Given the defined effect of a specified deposition on the plume a second spray produces a second shift to lower concentrations of equivalent width. The decrease in concentration persists at all subsequent downstream distances.

Figure 4 displays the influence of combining a fence and a water spray barrier located up- or downwind of one another on dilution and plume growth of a 1.4 specific gravity plume. Fences of 6 m height and 0 porosity were combined with water spray curtains which achieved entrainment velocities of 5 m/s and either 0 or 75 % deposition. The barriers were located alternatively at 20 m and 100 m downwind of the source area. In each case the downwind mitigation device reduces plume concentrations by only a modest amount. Certainly the first device encountered produces the majority of subsequent dilution. The fence is less effective downwind of a water spray curtain because at such a location the cloud height and advection velocities already exceed those at fence top. If the water spray is located within the wake of the fence, it may only add marginally to an already enhanced entrainment rate. Similar calculations performed for a 4.0 specific gravity plume produce very similar but somewhat larger dilutions.

#### INFLUENCE OF SIDE-WALL BARRIERS AROUND THE SOURCE LOCATION

The effect of lateral fences located either side of the source area and extending downwind to a fence were examined using the depth-integrated program, FENCE. The same generic API spill conditions were utilized as before. Calculations were performed for a region extending about 40 m upwind and 700 m downwind of the source center. The fence was located 20 m downwind of the source downwind edge, and any lateral barriers were located 10 m apart. Figure 5, 6 and 7 display the transient growth, advection and dilution of a continuous source of 1.4 specific gravity released in a 5.6 m/s wind at times 50, 100, 150, 200, 300 and 550 seconds after initial source release. Notice the transient appearance of a gravity head which eventually leaves the calculation domain downwind. Given the continuous nature of the source, the plume concentrations, height and width all approach asymptotic values for all distances displayed for times of 550 seconds.



A 6 m high fence of 0 % porosity produces dramatic plume growth at the fence followed by some density driven plume collapse; however, the plume widths for distances less than 600 m are somewhat narrower. The greater fence height wind speeds excite greater dilution rates in the fence wake.

Finally, the figures display the influence of lateral barriers about the source area which restrict initial lateral growth. Plumes are mixed to about the same height; hence, dilution is only marginally reduced. By the time the plume reaches distances of 700 m downwind, plume widths have asymptotically approached no-lateral-barrier conditions, and plume dilutions are essentially the same as without lateral barriers.

Figure 8 summarizes the asymptotic distributions of concentration, plume width and plume height which result at long times. This figure also displays the effect of 50 % fence porosity on wake development.

## CONCLUSIONS

Fence and water spray curtain field effects on plume dilution have now been measured for a wide range of laboratory and field conditions. These measurements suffice to calibrate simple box and depth-integrated numerical models. Calculations with such models for a range of hypothetical barrier configurations permit the designer to estimate the probable value of alternative arrangements. Superposition of the dilutions produced by barriers acting far enough apart to be considered independent suggests that such geometries are not as efficient together as when installed alone. Dilutions will increase, but total dilutions will not equal the sum of each acting alone. These calculations do not, however, provide any guidance concerning the use of fences and sprays constructed directly next to one another. For example, a fence might be used effectively to divert a plume into a smaller but more energetic water spray curtain.

## Acknowledgements

The authors wish to thank EXXON Research and Engineering Company, Florham Park, New Jersey, and the Gas Research Institute, Chicago, Illinois (Contract No. N00014-88-K-0029), for support of research related to this paper.

## References

API, 1989, "Effect of Homogeneous and Heterogeneous Surface Roughness on Heavier-Than-Air Gas Dispersion," Volume 1, American Petroleum Institute Publication No. 4491, Health and Environmental Sciences Department, Washington, D.C., 354 pp.

Andreiev, G., Meroney, R. N., and Neff, D. E., 1983, "Heat Transfer Effects During Cold Dense Gas Dispersion," for Gas Research Institute, Report GRI 83/0082, 224 pp.

Atallah, S. Guzman, E. and Shah, J.N., 1988, "Water Spray Barriers for LNG Vapor Mitigation," Gas Research Institute Topical Report, GRI Contract No. 5087-254-1575, Chicago, Illinois, 43 pp.

Atallah, S. Guzman, E. and Shah, J.N., 1989, "Vapor Fences for LNG Vapor Mitigation," Gas Research Institute Topical Report, GRI Contract No. 5087-254-1575, Chicago, Illinois, 30 pp.

Blewitt, D.N., Yohn, J.F., Koopman, R.P., Brown, T.C., and Hague, W.J., 1987, "Effectiveness of Water Sprays on Mitigating Anhydrous Hydrofluoric Acid Releases," Proceedings of International Conference on Vapor Cloud Modeling, CCPS, Cambridge, MA, 2-4 November, pp. 155-180.

Heskestad, G., Meroney, R.N., Kothari, K.M. and Neff, D.E., 1983, "Effectiveness of Water Spray Curtains in Dispersing LNG Vapor Clouds," Proceedings of AGA Transmission Conference, Seattle Washington, May 2-4, 1983, 40 pp.

Meroney, R. N. 1984, "Transient Characteristics of Dense Gas Dispersion; Part I: A Depth-Averaged Numerical Model," J. of Hazardous Materials, Vol. 9, pp. 139-157.

Meroney, R.N., 1986, "Guideline for Fluid Modeling of Liquefied Natural Gas Cloud Dispersion - Vol. II:," Technical Support Document, Final Report for Gas Research Institute, Report GRI86/0102.2, 262 pp.

Meroney, R. N. and Lohmeyer, A., 1982, "Gravity Spreading and Dispersion of Dense Gas Clouds Released Suddenly into a Turbulent Boundary Layer," for Gas Research Institute, GRI Report 82/0025, 220 pp.

Meroney, R.N., Neff, D.E., and Heskestad, G., 1984, "Wind-tunnel Simulation of a U.K. Health and Safety Executive Water Spray Curtain Dense Gas Dispersion Tests," J. of Boundary Layer Meteorology, Vol. 28, pp. 107-119.

Meroney, R. N. and Lohmeyer, A., 1984, "Prediction of Propane Cloud Dispersion by a Wind-Tunnel-Data Calibrated Box Model," J. of Hazardous Materials, Vol. 8, pp. 205-221.

Meroney, R.N., Neff, D.E., Shin, S.H., Steidle, T.C., Tan, T.Z., and Wu, G., 1988, "Analysis of Vapor Barrier Experiments to Evaluate their Effect as a Means to Mitigate the HF Cloud Concentration", for Exxon Research and Engineering, Florham Park, New Jersey, CSU Contract No. 29-7330, CER88-89RNM-DEN-SHS-TCS-TZT-GW-1, 200 pp.

Meroney, R.N. and Neff, D.E., 1985, "Numerical Modeling of Water Spray Barriers for Dispersing Dense Gases," J. of Boundary Layer Meteorology, Vol. 32, pp. 233-247.

Meroney, R.N. and Shin, S.H., 1991, "Numerical Simulation of the Mitigation of HF Cloud Concentrations by Means of Vapor Barriers and Water Spray Curtains," Proceedings of International Conference and Workshop on Modeling and Mitigating the Consequences of Accidental Releases of Hazardous Materials, Center for Chemical Process Safety, AIChE, New York, pp. 431-442.

Neff, D.E. and Meroney, R.N., 1986, "LNG Vapor Barrier and Obstacle Evaluation, Wind-tunnel Prefield Test Results", for Lawrence Livermore Laboratory, Contract No. 8432705, FMWEP85-86RNM3.

Puttock, J.S., Blackmore, D.R., and Colenbrander, G.W., 1982, "Field experiments on dense gas dispersion," J. Haz. Mat., Vol. 6, pp. 13-41.

Shin, S.H. and Meroney, R.N., 1991, "Wind Tunnel Model Validation for Vapor Dispersion from Vapor Detention System," Proceedings of International Conference and Workshop on Modeling and Mitigating the Consequences of Accidental Releases of Hazardous Materials, Center for Chemical Process Safety, AIChE, New York, pp. 369-384.

## List of Symbols

$C_D$	Fence dilution coefficient
H	Fence height
Q	Source strength
P	Fence porosity
Ri.	Richardson number = $(g'H/u_*^2)$
SG	Specific gravity
U	Wind speed
$U_{10}$	Reference wind speed at a 10 meter height
$U_f$	Plume frontal velocity
$u_*$	Friction velocity
$w_e$	Entrainment velocity
x	Downwind distance
$x_f$	Fence location
Z <sub>0</sub>	Surface roughness

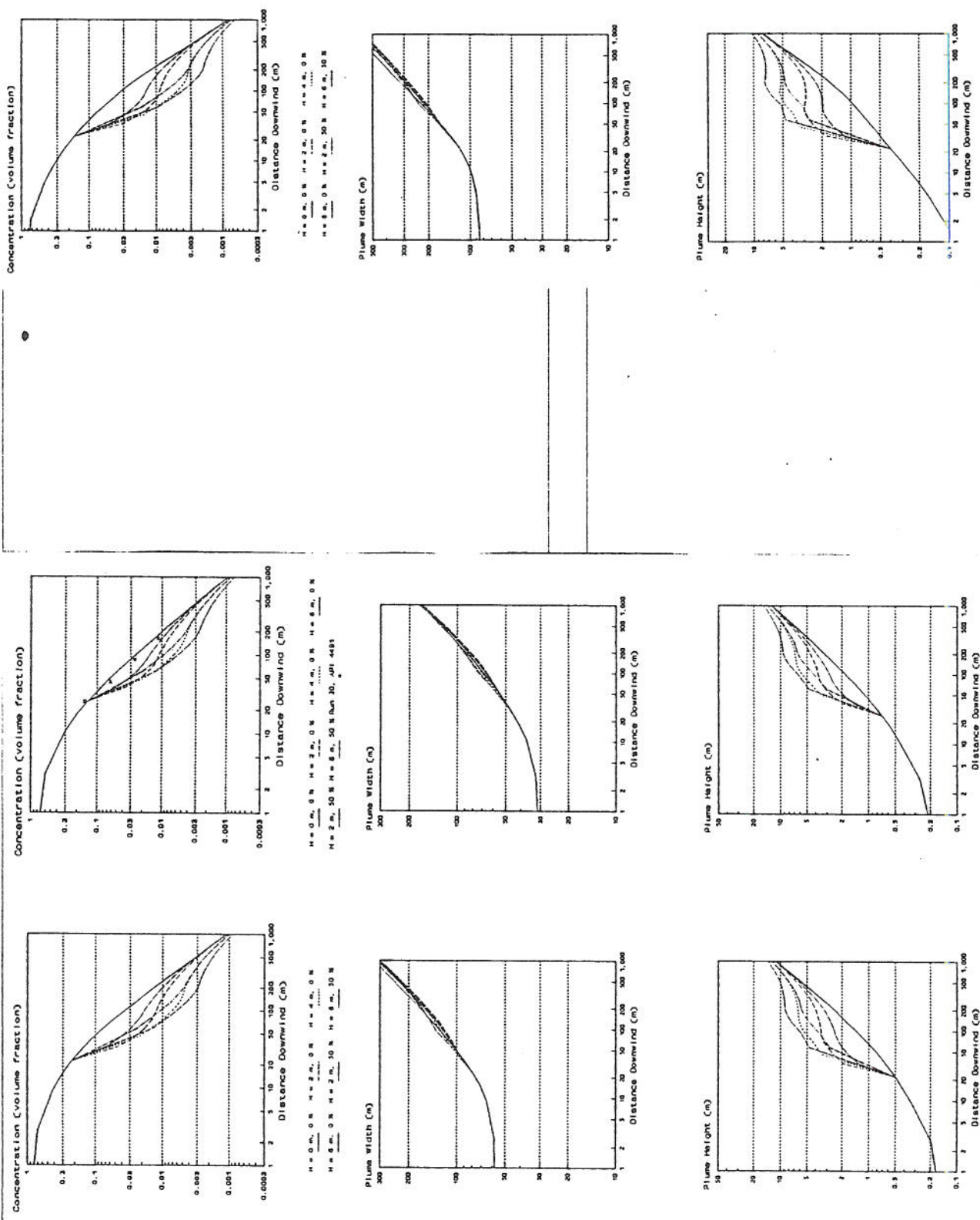


Figure 1:

Numerical box-model predictions of plume dilution, width and height for wind speeds of 3 m/s (left column) and 5.6 m/s (right column). Plume source strength  $Q = 11.14 \text{ m}^3/\text{s}$ , specific gravity  $SG = 1.4$ , and source width  $W = 5 \text{ m}$ . Fence heights  $H = 0, 2, 4$  and  $6 \text{ m}$  placed at  $x_f = 20 \text{ m}$ .

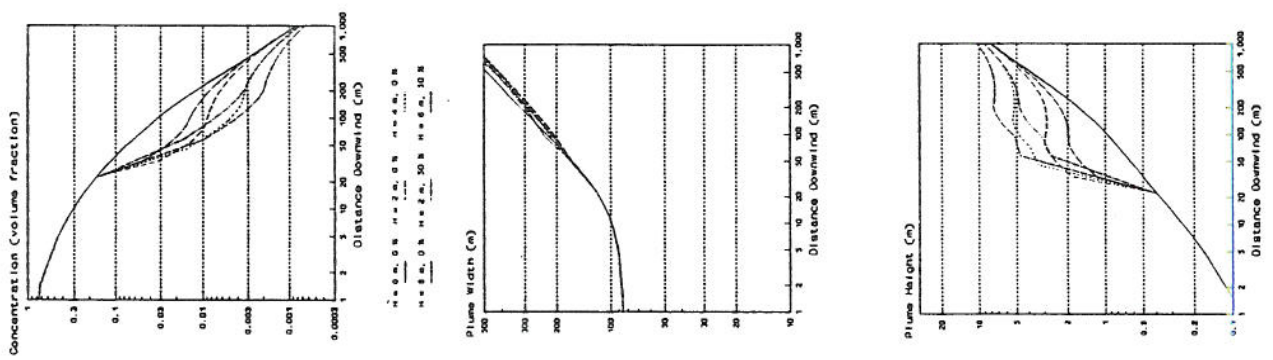


Figure 2:

Numerical box-model predictions of plume dilution, width and height for a wind speed of 3 m/s. Plume source strength  $Q = 11.14 \text{ m}^3/\text{s}$ , specific gravity  $SG = 4.0$ , and source width  $W = 5 \text{ m}$ . Fence heights  $H = 0, 2, 4$  and  $6 \text{ m}$  placed at  $x_f = 20 \text{ m}$ .



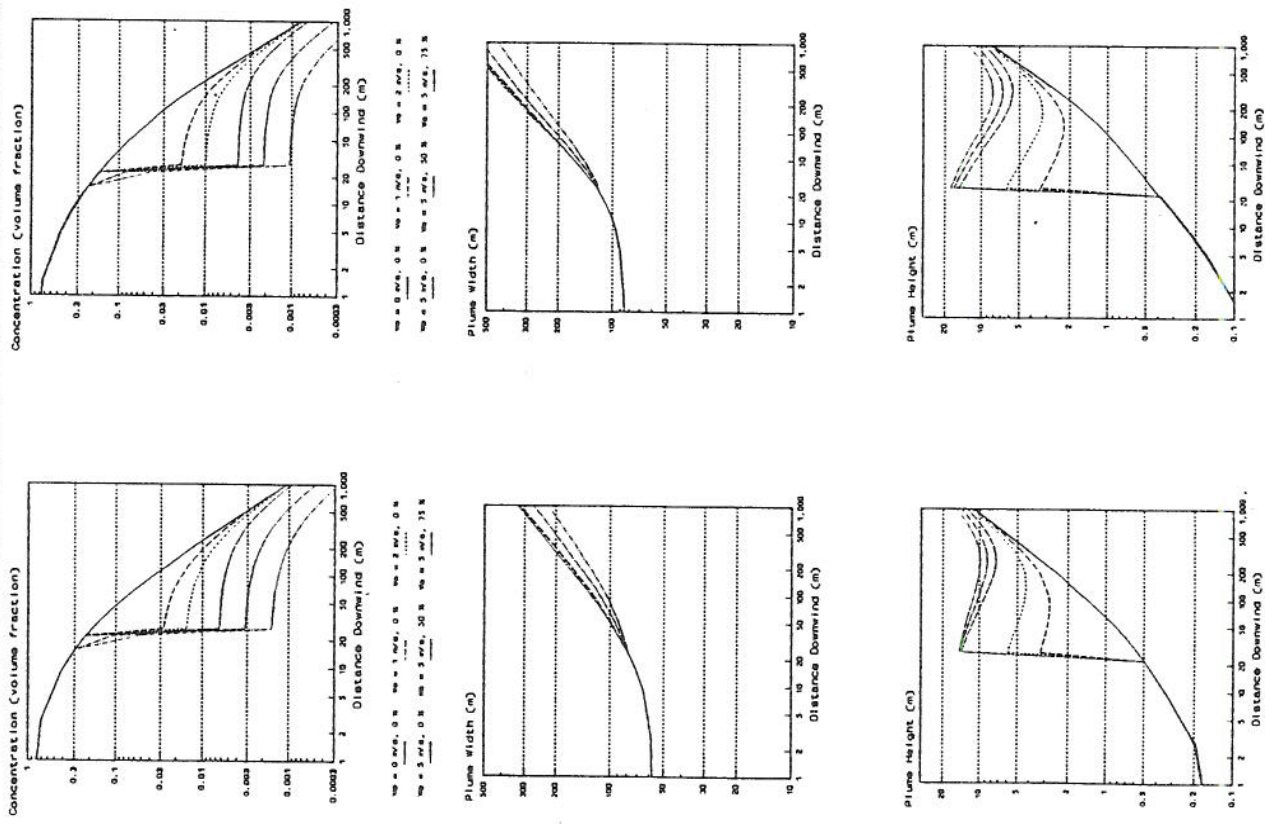


Figure 3: Numerical box = model predictions of plume dilution, width and height for a wind speed of 3 m/s. Plume source strength  $Q = 11.14 \text{ m}^3/\text{s}$ , specific gravity  $SG = 1.4$  (left column) and 4.0 (right column). Water sprays with entrainment velocities  $w_e = 0, 2, 4$  and 5 m/s placed at  $x_r = 20 \text{ m}$ .

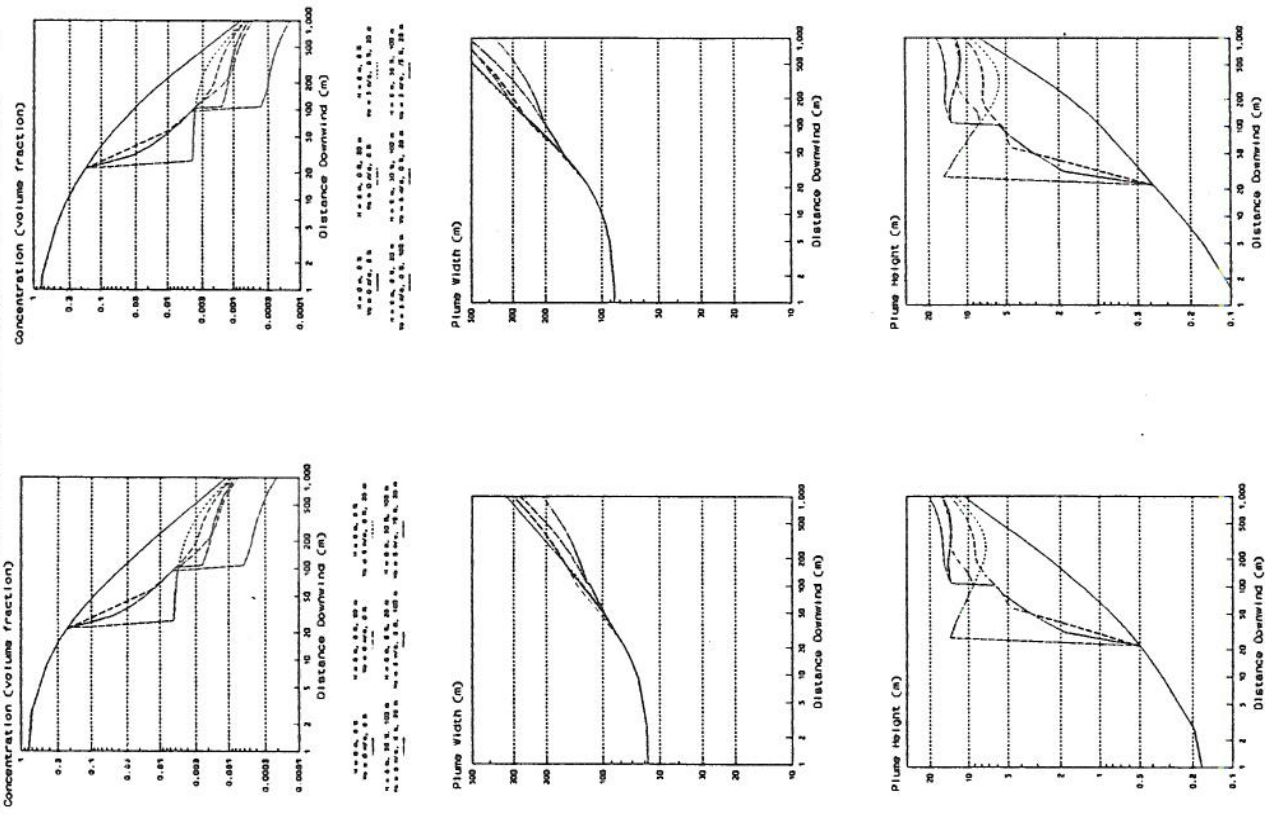


Figure 4: Numerical box = model predictions of plume dilution, width and height for a wind speed of 3 m/s. Plume source strength  $Q = 11.14 \text{ m}^3/\text{s}$ , specific gravity  $SG = 1.4$  (left column) and 4.0 (right column). Water sprays with entrainment velocities  $w_e = 0$  or 5 m/s and fences with height  $H = 0$  or 6 m were placed at  $x_r = 20$  m and/or 100 m.

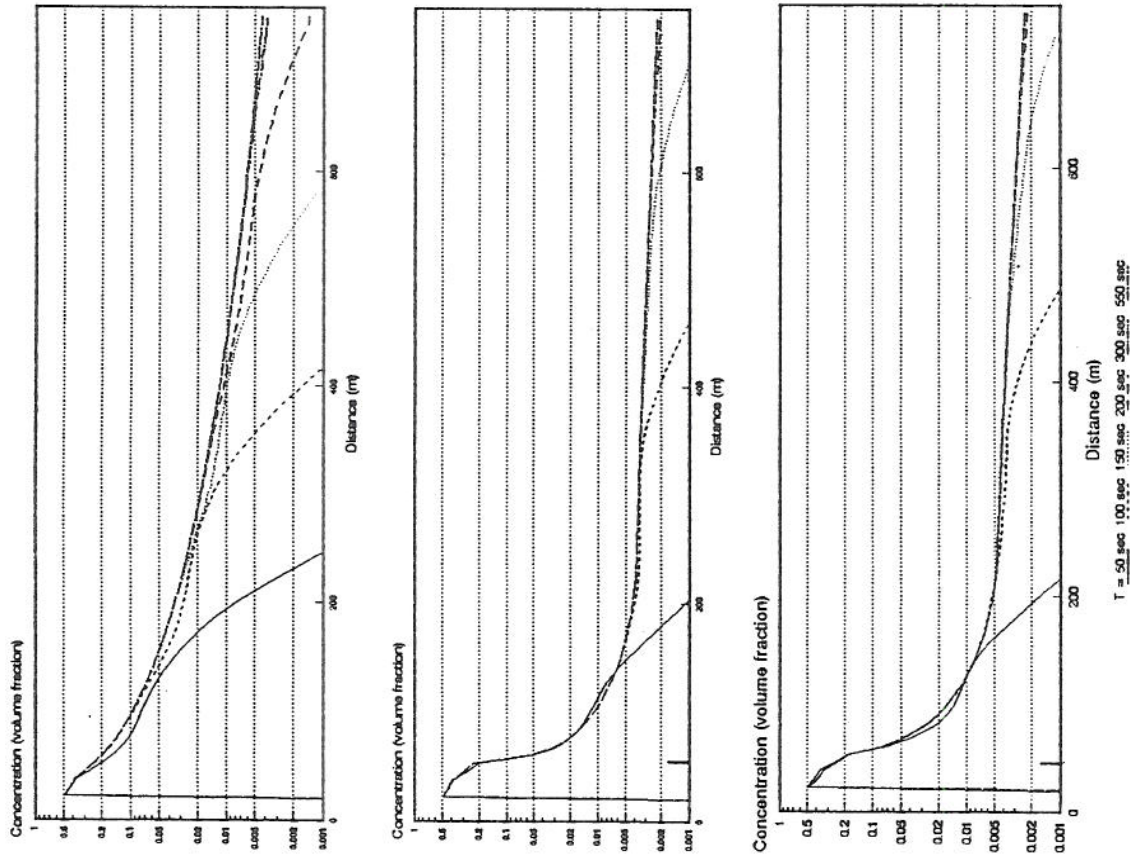


Figure 5: Numerical depth-integrated predictions of plume dilution for a wind speed of 5.6 m/s. Plume source strength  $Q = 11.14 \text{ m}^3/\text{s}$ , and specific gravity  $SG = 1.4$ . Fence height  $H = 0$  m (top figure) or 6 m (middle and bottom figures) were placed at  $x_f = 20$  m. Lateral plume spread over the source may be limited to 10 m (bottom figure).

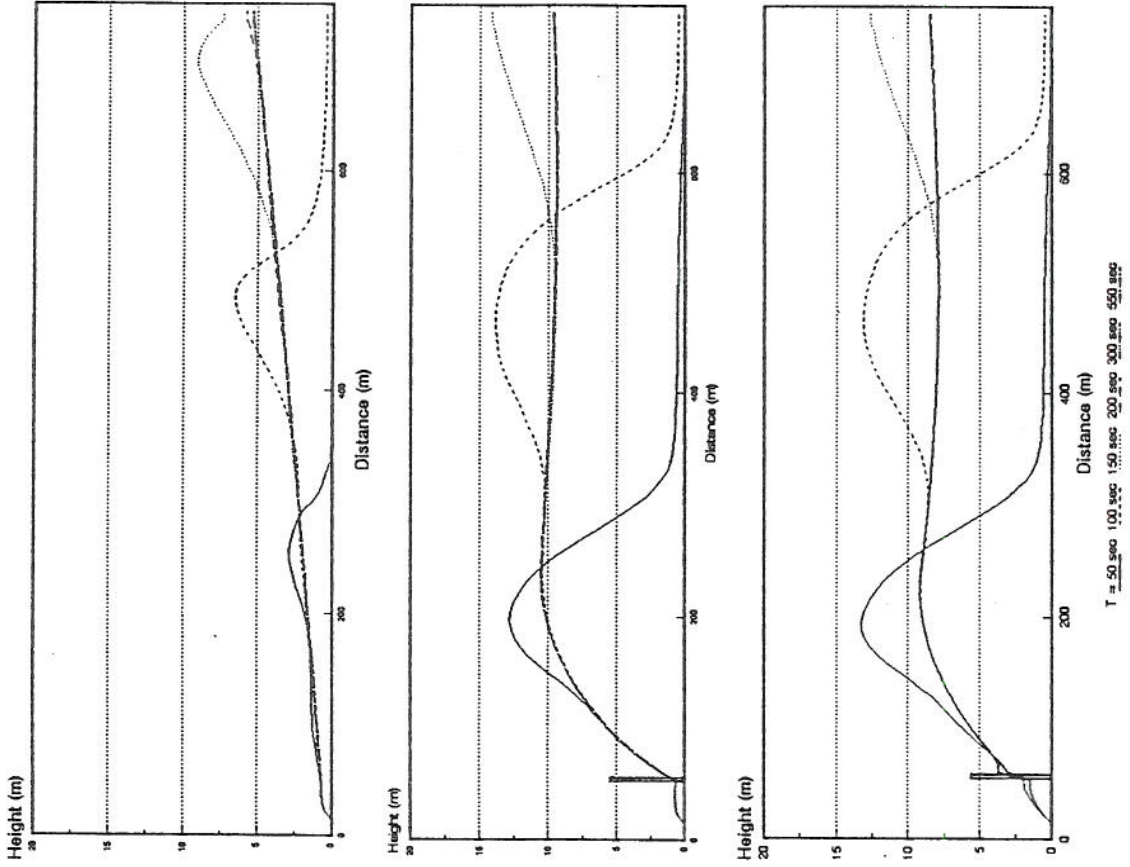
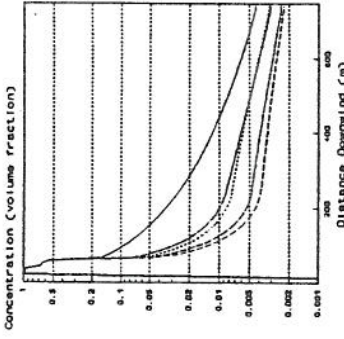


Figure 6: Numerical depth-integrated predictions of plume height for a wind speed of 5.6 m/s. Plume source strength  $Q = 11.14 \text{ m}^3/\text{s}$ , and specific gravity  $SG = 1.4$ . Fence height  $H = 0$  m (top figure) or 6 m (middle and bottom figures) were placed at  $x_f = 20$  m. Lateral plume spread over the source may be limited to 10 m (bottom figure).





$U = 5.6 \text{ m/s}$   
 $Q = 11.14 \text{ m}^3/\text{s}$   
 $H = 20 \text{ m}$   
 $SG = 1.4$   
 $P = 0$   
 $x_r = 0 \text{ m}$   
 $x_r = 6 \text{ m}$   
 $x_r = 10 \text{ m}$

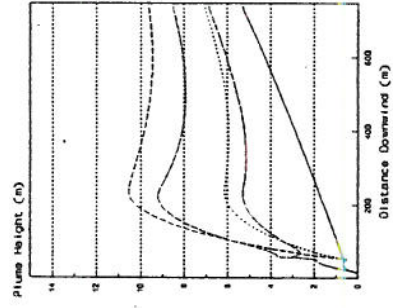
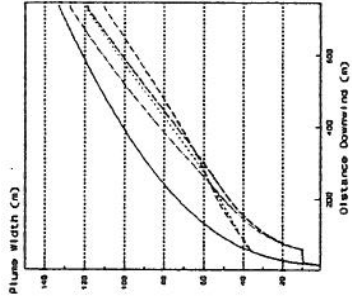
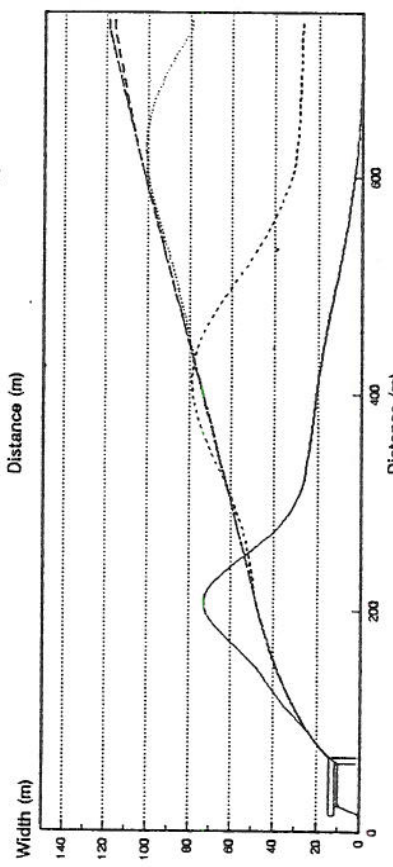
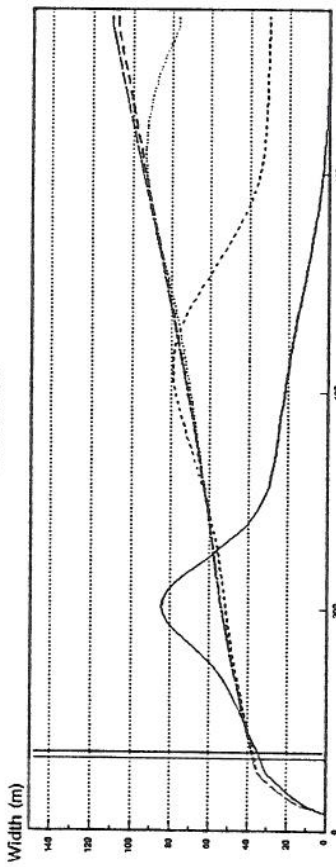
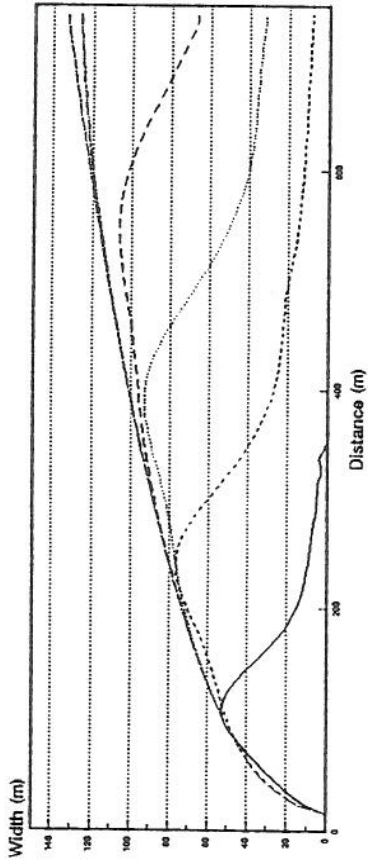


Figure 8: Numerical depth-integrated predictions of plume dilution, height and width for a wind speed of 5.6 m/s from a continuous small-area source after extended times. Plume source strength  $Q = 11.14 \text{ m}^3/\text{s}$ , and specific gravity  $SG = 1.4$ . Fence heights  $H = 0$  or  $6 \text{ m}$  at  $x_r = 20 \text{ m}$ , fence porosity  $P = 0$  or  $50 \%$ , and source enclosure width is unlimited or  $10 \text{ m}$ .



$T = 50 \text{ sec}$   
 $T = 100 \text{ sec}$   
 $T = 150 \text{ sec}$   
 $T = 200 \text{ sec}$   
 $T = 300 \text{ sec}$   
 $T = 500 \text{ sec}$

Figure 7: Numerical depth-integrated predictions of plume width for a wind speed of 5.6 m/s. Plume source strength  $Q = 11.14 \text{ m}^3/\text{s}$ , and specific gravity  $SG = 1.4$ . Fence height  $H = 0 \text{ m}$  (top figure) or  $6 \text{ m}$  (middle and bottom figures) were placed at  $x_r = 20 \text{ m}$ . Lateral plume spread over the source may be limited to  $10 \text{ m}$  (bottom figure).